

Noise effects in intrinsic laser polarization switching

K. Al Naimee,^{1,2} I. Leyva,³ I. P. Mariño,³ R. Meucci,¹ and F. T. Arecchi^{1,4}

¹*CNR-Istituto Nazionale di Ottica Applicata, Largo Enrico Fermi 6, 50125 Florence, Italy*

²*Physics Department, College of Science, University of Baghdad, Baghdad, Iraq*

³*Universidad Rey Juan Carlos, c/Tulipán s/n, 28933 Móstoles, Madrid, Spain*

⁴*Physics Department, University of Florence, Italy*

(Received 21 February 2008; published 3 June 2008)

A quasi-isotropic CO₂ laser near the resonant condition can present bistability in the polarization state, with spontaneous flips between two orthogonal linear polarization eigenmodes. In this work, we explore the role of the pump and noise on the polarization dynamics, showing a transition from stable to bistable states and the presence of coherence resonance.

DOI: 10.1103/PhysRevA.77.063803

PACS number(s): 42.60.Mi, 42.65.Sf

I. INTRODUCTION

Laser dynamics is usually explored considering the main variable, the electric field, as a scalar, since in most laser systems the polarization is fixed by anisotropies of the cavity. However, in cavities without any selection of a preferred polarization, the study of the dynamics must account for the vector nature of the electric field. Due to this additional degree of freedom, vectorial laser systems can display polarization bistability under certain conditions.

Extensive research on polarization has been developed for solid-state lasers [1–3], due to their great interest in applications, especially in the case of vertical cavity surface emitting lasers (VCSEL) [4]. Polarization of a laser beam has crucial effects in material processing, and therefore it is important to control it also in gas lasers. For laser cutting, operating a beam with circular polarization is highly desirable and it is achieved by means of a phase shifter which converts a fixed linear polarization to circular polarization. In stable-unstable resonators, radiation exhibits polarization jumps especially when operated near the optimal conditions of high pumping. In the presence of polarization jumping, the role of the external phase retarder is lost. In lasers with folded cavities, jumps between two linear polarization directions are eliminated by the use of a polarization locking mirror which strongly selects the *s* polarization.

For the case of a quasi-isotropic laser, the polarization dynamics has been investigated in several works, pointing out the role played by the material variables in the selection of the polarization state [5–13]. In previous works, we have extended this theoretical frame to the study of laser dynamics driven by more complicated level structures [14], including also spatial degrees of freedom [15]. Furthermore, we have explored the potential applications of this bistable dynamics, showing how the polarization can be controlled by means of feedback, so that information can be encoded in the polarization without affecting the total intensity [16]. Ultimately, we have proved that this information can be transmitted to another laser by means of synchronization [17].

Thus far, the effects of noise on the bistable polarization dynamics of a laser has not been extensively studied. In Ref. [3] experimental evidence of stochastic resonance in the polarization state of VCSELs is given. In Refs. [18,19] experi-

mental and theoretical studies of coherence resonance are presented in a VCSEL with polarization bistability induced by time-delayed feedback.

In this work, we experimentally and numerically study the effects of noise in the polarization dynamics of an isotropic CO₂ laser with noise-induced polarization bistability, including experimental evidence of coherence resonance (CR). We observe CR in a quasisymmetric optical system with a bistability based only on symmetry breaking due to residual anisotropies.

II. EXPERIMENTAL RESULTS

The experimental setup is shown in Fig. 1. It consists of a quasi-isotropic CO₂ laser, with a Fabry-Perot optical resonator defined by a totally reflective mirror and a partially reflective mirror mounted on a piezoelectric transducer (PZT) in order to control the laser detuning. The laser tube is terminated by an antireflection coated ZnSe window. Particular attention has been devoted to the insertion of two electrodes in the laser tube for preserving the cylindrical geometry of the discharge. The cavity length is 550 mm while the discharge length is 420 mm. The active medium is a mixture of 82% He, 13.5% N₂, and 4.5% CO₂ gases and it is pumped by a dc discharge current. The laser beam is directed toward the infrared camera (PyrocamIII) after passing through a linear polarizer fixed at 45° with the beam direction. The reflected beam from the polarizer is directed to a fast-response room-temperature mercury-cadmium-telluride (MCT) detector

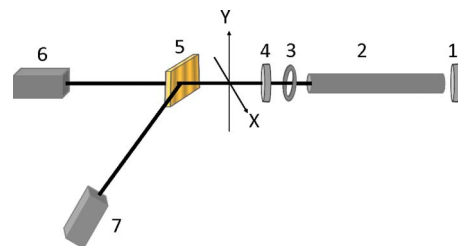


FIG. 1. (Color online) Experimental setup: (1) High reflection mirror, (2) CO₂ laser tube, (3) iris diaphragm, (4) output coupler, (5) wire grid polarizer (beam splitter), (6) infrared camera, (7) MCT detector.

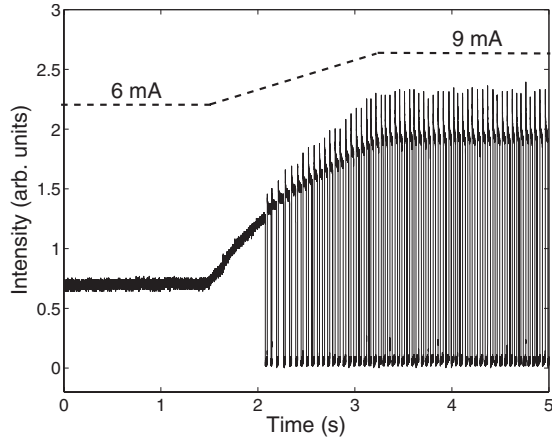


FIG. 2. Time sequence of polarization switching at different pump levels. Transition between the low (6 mA) to high (9 mA) discharge current (dashed line). Jumps occur between the two polarization states. Zero intensity corresponds to the state blocked by the detection setup.

coupled with a LeCroy 500 MHz digital oscilloscope.

To examine the reliability of the polarization dynamics close to resonant cavity conditions, the discharge current is slowly changed between an initial value (6 mA) where no switches between polarizations are observed, to a high value where a fast switching occurs (9 mA). Figure 2 shows this transition between the stable condition and the bistable one where the switching spontaneously occurs. This means that increasing the pump induces polarization bistability in the laser when it is in resonant condition. In previous experiments [14,16], we had reported this bistable condition, but its dependence on the pump level is given here.

The role of noise has also been investigated by adding to the discharge current a white noise with variable level of variance σ . Noise is added when the polarization state is stable at a low pump level. The switching condition between polarization states is also achieved in this way. The bistability appears when the noise signal (rms value) is around 5% of the steady-state value. In Fig. 3 we show the polarization jumps induced by noise with small σ [Fig. 3(a)], and higher σ [Fig. 3(b)], where it appears that the frequency of the jumps increases.

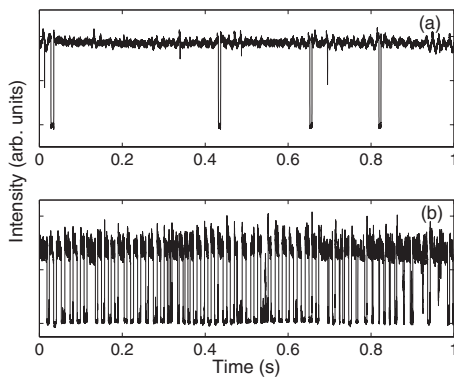


FIG. 3. Experimental laser intensity for the same discharge current of 6 mA with two levels of noise: (a) $\sigma=103$ mV, (b) $\sigma=600$ mV.

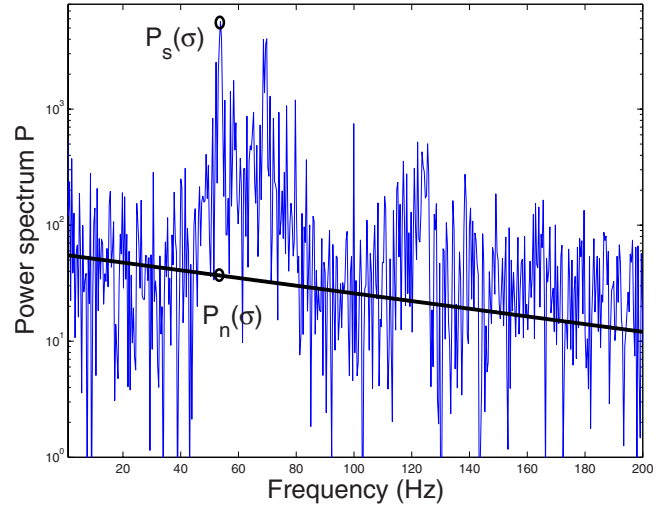


FIG. 4. (Color online) Semilogarithmic plot of the power spectrum of the experimental signal plotted in Fig. 3(b) (blue line), as well as the corresponding extrapolated noise background power spectrum (black line). The relevant points used in the calculation of the SNR are indicated as $P_s(\sigma)$ and $P_n(\sigma)$.

This polarization bistability driven by noise shows evidence of coherence resonance, here reported for non-solid-state lasers. In order to obtain quantitative measure of this phenomenon, we study the signal-to-noise ratio (SNR) of the power spectrum of a polarized intensity component for increasing values of the noise variance σ , measured in mV. This magnitude is defined as $\text{SNR}(\sigma) = 10 \log_{10}[P_s(\sigma)/P_n(\sigma)]$, where $P_s(\sigma)$ is the maximum of the power spectrum of the experimental signal and $P_n(\sigma)$ is the corresponding value of the power spectrum for the extrapolated noise background. In order to clarify this measurement, in Fig. 4 we plot an example of this experimental signal power spectrum P corresponding to the signal plotted in Fig. 3(b), as well as the corresponding extrapolated noise background power spectrum, showing the relevant points $[P_s(\sigma), P_n(\sigma)]$ used in the calculation of the $\text{SNR}(\sigma)$. As it can be seen in Fig. 5, a maximum of the $\text{SNR}(\sigma)$ is achieved for $\sigma \approx 600$ mV, corresponding to the situation presented in Fig. 3(b).

III. MODEL AND NUMERICAL RESULTS

Our numerical approach to the described situation is based on the theory of the isotropic laser developed in Ref. [6], where the optical coherences between upper levels are included as the source of competition between the orthogonally polarized fields. This theory was developed for the simplest case of rotational levels ($J=1 \rightarrow J=0$), but it can be generalized to account for the dynamics of systems with a more complex level structure (as HeNe, XeNe [11], and CO₂ lasers [14]), by fitting an effective value of the coherence decay rate. The model considers only two kinds of possible transitions, and therefore the population splits in two ensembles. The electric and matter polarization fields can then also be decomposed in orthogonal components which interact through the coherences between the upper sublevels.

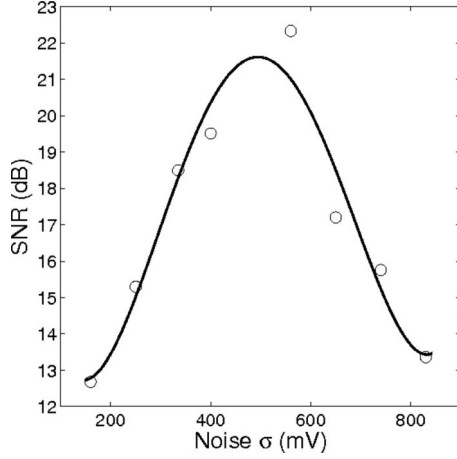


FIG. 5. Signal-to-noise ratio (SNR) of the maximum peak of the power spectrum of the polarized laser intensity as a function of the rms noise value applied to the pump.

In this competitive dynamics, the anisotropy due to the cavity detuning can decide the polarization of the laser [9,11,14]. However, this anisotropy disappears at resonance, as it is in our case. Additionally, our system is quasi-isotropic, and therefore the possible linear anisotropies are reduced to the unavoidable residual mechanical vibration, minimal misalignments or even nonuniform heating. All of these possible effects behave as an effective noise, that is at the base of the observed bistability. This behavior cannot be faithfully reproduced with a static linear loss parameter, which is the usual form in the literature [5]. Then, in our model the linear anisotropy parameter is included as a noise. Finally, the model reads as [5,14,16]

$$\begin{aligned}
 \dot{E}_R &= [\kappa(D_R - 1) + i\delta]E_R + (\kappa C - \alpha)E_L, \\
 \dot{E}_L &= [\kappa(D_L - 1) + i\delta]E_L + (\kappa C - \alpha)E_R, \\
 \dot{C} &= -\gamma_{\parallel} \left[C \left(1 + \frac{1}{4}(|E_L|^2 + |E_R|^2) \right) - \frac{1}{4}E_R E_L^* (D_R + D_L) \right], \\
 \dot{D}_R &= -\gamma_{\perp} \left[D_R(1 + |E_R|^2) - r + \frac{1}{2} \left(D_L |E_L|^2 + \frac{3}{2} (E_R E_L^* C^* \right. \right. \\
 &\quad \left. \left. + E_L E_R^* C) \right) \right], \\
 \dot{D}_L &= -\gamma_{\perp} \left[D_L(1 + |E_L|^2) - r + \frac{1}{2} \left(D_R |E_R|^2 + \frac{3}{2} (E_R E_L^* C^* \right. \right. \\
 &\quad \left. \left. + E_L E_R^* C) \right) \right], \tag{1}
 \end{aligned}$$

where $E_R(t), E_L(t)$ are the slowly varying electric fields, $D_R(t)$ and $D_L(t)$ are the respective population inversions. Subscripts R and L stand for right and left, respectively, indicating that a circularly polarized basis is adopted for the fields. The losses are $\kappa = -c \ln(R_1 R_2) / 4L = 6.74 \times 10^6 \text{ s}^{-1}$. In our low pressure CO_2 laser, the polarization decay is

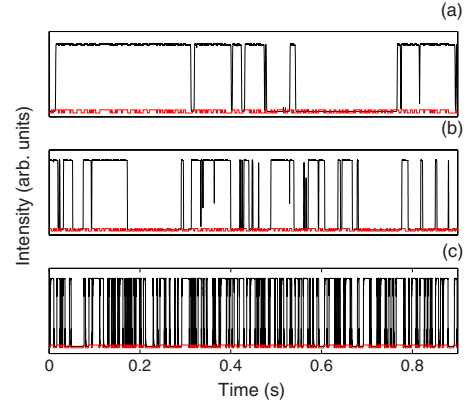


FIG. 6. (Color online) Numerically generated temporal evolution of the Y polarized intensity component (black lines) and linear anisotropies parameter α (red lines), for $\beta=0.01$, $\alpha_0=0.002$ and several values of the pump parameter: (a) $r_0=1.02$, (b) $r_0=1.06$, and (c) $r_0=1.09$.

$\gamma_{\perp} = 4.4 \times 10^8 \text{ s}^{-1}$, the inversion decay rate is $\gamma_{\parallel} = 1.95 \times 10^5 \text{ s}^{-1}$, and the coherence decay rate is fitted to $\gamma_c = \gamma_{\parallel}$ [14]. Therefore, the experimental system corresponds to a class B laser, and then the polarization matter variables have been adiabatically eliminated. $C(t)$ represents the optical coherence between the upper sublevels in the case of the transition from a state $J=1$ to $J=0$. In a matrix density description, C corresponds to the off-diagonal matrix elements coupling different angular momentum states of the upper level [5].

The parameter δ represents the detuning between the cavity and the atomic transition frequencies. In our numerical study, we fit $\delta=0$ since in the experiment the laser remains close to resonant condition. Parameter $\alpha(t)$ represents the linear anisotropies in the losses with respect to the laser eigendirections (in the following XY axes, see Fig. 1). As mentioned above, in our model the linear anisotropy parameter is included as $\alpha(t) = \kappa \alpha_0 \epsilon(t)$, where α_0 is a small perturbation and ϵ is a dichotomous noise varying in the interval $[-1, 1]$, with a characteristic time fitted to the observed experimental polarization flips [14].

The parameter $r(t)$ stands for the pump strength normalized to its threshold value. In order to reproduce both experimental forms in which the noisy pump is applied to our system, we write this parameter as $r(t) = r_0(1 + \beta \xi)$, where r_0 is the mean value of the pump, ξ is a uniform white noise in the interval $[-1, 1]$, and β is the maximum noise amplitude. Here ξ accounts both for the inner noise of the pump, natural to any experiment, as well as for the additional noise applied through the discharge current, as done in the experiment.

Notice that for a better comparison with the experiment, in Figs. 6 and 7 the fields are written in the orthogonal basis $[E_X = (E_L + E_R) / \sqrt{2}, E_Y = i(E_L - E_R) / \sqrt{2}]$, corresponding to the eigendirections in the laser.

Numerical simulations have been carried out in order to analyze the effects of the noise in the pump parameter in the polarization switching induced by the cavity losses. We have observed that for a fixed value of β , depending on the mean pump value r_0 (or, what is equivalent, on the laser power), the system changes from a stable polarization to a bistable

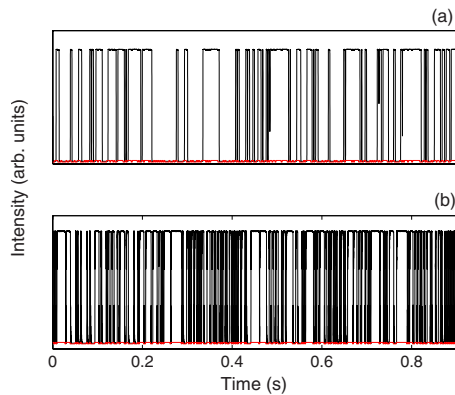


FIG. 7. (Color online) Numerically generated temporal evolution of the Y polarized intensity component and parameter α , for constant pump $r_0=1.08$ and two values of β : (a) $\beta=0.01$, (b) $\beta=0.03$.

condition of polarization switching. Thus, depending on the available energy, the linear anisotropies in the cavity losses can induce polarization jumps or not. In Fig. 6 we give numerical results of the temporal evolution of the Y polarized intensity component together with the temporal evolution of the parameter α (magnified for better observation), for increasing values of the mean pump parameter r_0 , while β is constant during the simulation with a value of about 1% of the global pump. It can be noticed that α is about 0.1% of the total losses κ , which fits well with an effective noise. We see that very close to the lasing threshold the polarization rarely switches [Fig. 6(a)], but for increasing values of r_0 , the jumps occur more often [Fig. 6(b)] and finally, for sufficiently high values of r_0 [Fig. 6(c)], the linear anisotropies in the cavity losses guide completely the transitions between the two polarizations. This can be compared with its experi-

mental counterpart, Fig. 2, where the experimental route from low to high energy is plotted.

This model also reproduces the experimental response of the polarization flips when increasing white noise is added to the pump, shown in Fig. 3. The equivalent numerical results can be seen in Fig. 7, where the Y intensity is plotted for two values of the maximum noise amplitude β (1% and 3%) with r_0 fixed. Unfortunately, in spite of the fact that it reproduces most of the observed features, it is clear that our model is not able to reproduce the coherent resonance observed in the experiment, since the model must fit the unknown cavity anisotropies through binomial noise in the α parameter. Therefore, for a certain value of α , the noise can induce polarization flips but they are not coherent unless the perturbation in the losses is periodic.

IV. CONCLUSIONS

In conclusion, we have experimentally shown the noise induced transition from monostable to bistable polarization of an isotropic laser. For certain values of the noise, the polarization flips are maximally coherent. This is one of the few experimental evidences of coherent resonance in non-feedback bistable optical systems. A model based on vectorial Maxwell-Bloch equations with optical coherences reproduces most of the results.

ACKNOWLEDGMENTS

I.L. and I.P.M. acknowledge financial support by Universidad Rey Juan Carlos and Comunidad de Madrid under Contracts No. URJC-CM-2006-CET-0643 and No. URJC-CM-2007-CET-1601, and by the Spanish Ministry of Education and Science under Contract No. FIS2006-08525. K.A.N. acknowledges ICTP for financial support in the framework of the TRIL project.

-
- [1] Y. C. Chen and J. M. Liu, *Appl. Phys. Lett.* **46**, 16 (1985).
 [2] See, for instance, M. San Miguel, Q. Feng, and J. V. Moloney, *Phys. Rev. A* **52**, 1728 (1995); O. Hess and T. Kuhn, *ibid.* **54**, 3347 (1996).
 [3] G. Giacomelli, F. Marin, and I. Rabbiosi, *Phys. Rev. Lett.* **82**, 675 (1999).
 [4] Z. George Pan, Shijun Jiang, Mario Dagenais, Robert A. Morgan, Keisuke Kojima, Moses T. Asom, Ronald E. Leibenguth, Gregory D. Guth, and Marlin W. Focht, *Appl. Phys. Lett.* **63**, 2999 (1993).
 [5] N. B. Abraham, M. D. Matlin, and R. S. Gioggia, *Phys. Rev. A* **53**, 3514 (1996).
 [6] G. C. Puccioni, M. V. Trantnik, J. E. Sipe, and G. L. Oppo, *Opt. Lett.* **12**, 242 (1987).
 [7] G. C. Puccioni, G. L. Lippi, and N. B. Abraham, *Opt. Commun.* **72**, 361 (1989).
 [8] N. B. Abraham, E. Arimondo, and M. San Miguel, *Opt. Commun.* **117**, 344 (1995).
 [9] For a review see G. M. Stephan and A. D. May, *Quantum Semiclass. Opt.* **10**, 19 (1998).
 [10] Yu. V. Loiko, A. M. Kulminskii, and A. P. Voitovich, *Opt. Commun.* **210**, 121 (2002).
 [11] M. D. Matlin, R. S. Gioggia, N. B. Abraham, P. Glorieux, and T. Crawford, *Opt. Commun.* **120**, 204 (1995).
 [12] C. Serrat, R. Vilaseca, G. J. de Valcárcel, and E. Roldán, *Phys. Rev. A* **56**, 2327 (1997).
 [13] Shulian Zhang and Ligang Fei, *Opt. Eng.* **45**, 114201 (2006).
 [14] I. Leyva, E. Allaria, and R. Meucci, *Opt. Commun.* **217**, 335 (2003).
 [15] I. Leyva, E. Allaria, and R. Meucci, *Phys. Rev. A* **68**, 053806 (2003).
 [16] R. Meucci, F. Salvadori, I. Leyva, I. P. Mariño, K. Al Naimee, and M. Capo, *Opt. Commun.* **268**, 169 (2006).
 [17] I. P. Mariño, K. Al Naimee, F. Salvadori, M. Capo, R. Meucci, and F. T. Arecchi, *Opt. Commun.* **276**, 272 (2007).
 [18] K. Panajotov, M. Sciamanna, A. Tabaka, P. Mégret, M. Blondel, G. Giacomelli, F. Marin, H. Thienpont, and I. Veretennicoff, *Phys. Rev. A* **69**, 011801(R) (2004).
 [19] M. Arizleta Arteaga, M. Valencia, M. Sciamanna, H. Thienpont, M. López-Amo, and K. Panajotov, *Phys. Rev. Lett.* **99**, 023903 (2007).